DISTRIBUTION STATEMENT A. Approved for public release; distribution is unlimited.

Improved EM Tactical Applications through UAS-Enhanced High-Resolution Mesoscale Data Assimilation and Modeling

Teddy R. Holt
Naval Research Laboratory
Monterey, CA 93943-5502
phone: (831) 656-4740 fax: (831) 656-4769 e-mail: teddy.holt@nrlmry.navy.mil

Award Number: N0001414WX20290

LONG-TERM GOALS

The long-term goal of this project is to develop new and emerging analysis and forecast capabilities via improvements to environmental inputs to electro-magnetic (EM) tactical applications through Unmanned Aerial Systems (UAS) enhanced high-resolution mesoscale data assimilation and modeling. These capabilities will be achieved through the formulation, testing, evaluation, and demonstration of an environmental data assimilation and prediction system designed to quantify the UAS observation parameters, characteristics (e.g., vertical resolution), measurement strategies and assimilation approaches that provide the greatest benefit for high-resolution (grid increment of 5-km or less) atmospheric tactical-scale environmental forecasts. The goal is to focus on EM tactical applications and metrics in evaluating the performance of the system. This development will leverage current and emerging capabilities for: i) environmental data assimilation, ii) adjoint-based sensitivity and observation impact, iii) air-ocean coupled modeling, and iv) EM tactical decision aid systems. Observational results from field programs such as Trident Warrior 2013 (TW13) will also be leveraged to build, test, and transition the prototype end-to-end (observation to tactical decision aid (TDA)) demonstration system. All meteorological inputs to the demonstration system will come from UAS platforms and sensors consistent with the present state-of-the-art; however, no specific operational UAS system will be targeted, transitioned or modified as part of this effort.

OBJECTIVE

The objective is to develop, validate, and transition new METOC capabilities within a high-resolution modeling system using advanced data assimilation of UAS data in order to achieve superior short and medium term forecasts of high-impact weather and EM-related parameters. We will use three crucial model components: i) the coupled atmospheric and oceanic components of the Coupled Ocean/Atmosphere Mesoscale Prediction System (COAMPS®[1]), ii) the 3D-variational (3DVAR) analysis schemes NAVDAS (NRL Atmospheric Variational Data Assimilation System) for the atmosphere and NCODA (Navy Coupled Ocean Data Assimilation) for the ocean and wave models, and iii) the COAMPS Adjoint observation impact system. COAMPS-OS®[1] will be used as the software interface for configuring COAMPS and the other system components to facilitate high-resolution coupled mesoscale forecasts. The COAMPS system includes an ocean circulation model, the Navy

[1] COAMPS® and COAMPS-OS® are registered trademarks of the Naval Research Laboratory.

Coastal Ocean Model (NCOM), which fully interacts with the nonhydrostatic atmospheric module. In addition, two different wave models are currently being implemented and tested: Simulating Waves Nearshore (SWAN) and Wavewatch III (WWIII), which will also be available for testing. NAVDAS is the Navy's state-of-the-art analyses system. The adjoint of the COAMPS forecast model and NAVDAS data assimilation systems have already been developed and linked together to provide a quantitative measure of the impact of individual observation types (e.g., radiosonde, aircraft, UAS, etc.) on the COAMPS forecast error. This observation impact capability has only recently become available for COAMPS and is one of the first such observation impact capabilities for a mesoscale modeling system developed anywhere.

Several key scientific objectives are identified in relation to the impact of the environment on EM propagation characteristics, particularly in the coastal marine atmospheric boundary layer (MABL): i) the time-varying 3-D structure of the MABL and its interaction and impact on EM propagation characteristics and ducting of EM energy, ii) the response of the MABL to the structure of the underlying SST, including SST gradients, and the impact on evaporative duct height calculations, on MABL refractive layers, and on larger-scale surface and MABL ducting phenomena, and iii) the most effective UAS observing strategies from an atmospheric model data assimilation perspective in order to accurately predict mesoscale weather and EM propagation conditions.

APPROACH

Our approach is to leverage prior investments in NRL-developed NAVDAS (including aircraft data assimilation), COAMPS, adjoint, and EM TDA technologies to produce a UAS-enabled, integrated, and automated on-scene system to support ASW, ASuW, and ISR mission planning and execution. Significant collaborations with other investigators developing and integrating UAS-based data and tools will be also leveraged. Collaborations with Scripps Institute of Oceanography (SIO), NSWC-Dahlgren, and other PMW-120 EM investigators will be pursued and help guide our sampling strategies, assure the UAS observations taken are in accord with NRL goals, and enhance synergistic development of UAS-based TDAs. Six specific technologies that will be developed, tested, and integrated in this project are i) tactical-scale data assimilation, ii) adjoint-based observation impact, iii) air-ocean coupled modeling, iv) EM tactical decision aid systems, v) software infrastructure, and vi) validation and verification of the end-to-end system.

WORK COMPLETED

Work that has been completed includes: i) testing and revising the UAS ScanEagle (SE) data processing software (v1.0) using quality-controlled SE UAS data, ii) analysis of COAMPS model performance during the TW13 observation campaign, iii) enhancements to and application of the COAMPS adjoint and tangent linear models toward assessment of the impact of SE data assimilation on COAMPS model error reduction

i) *ScanEagle data processing software development:*
Initial tests of SE data processing software operated during the TW13 observation campaign were evaluated, resulting in several software code improvements. The data assimilation algorithm designed to thin regions of dense observations was revised to prevent thinning of SE observations. Subsequent

distribution of a quality controlled version of the SE observation set from TW13 permitted the addition of quality control features within the SE data processing software.

ii) *Evaluation of COAMPS model performance during TW13*:
Experiments testing the impact of assimilated SE data on the coupled COAMPS-NCOM modeling system with NAVDAS 3D-Var data assimilation were re-run using quality-controlled SE data from TW13. Two model experiments were conducted: the modeling system operated with SE data assimilation (*UAS*) and the modeling system operated without SE data assimilation (*noUAS*). Evaluation of model forecasts included the use of the standard COAMPS post-processing model verification software as well as a package customized for comparison of TW13 model fields with SE observations and radiosonde measurements. Most model forecast evaluation involved grid 4 (Δx =1.33 km) of the nested grid domain (Figure 1), a region of 223 x 229 grid points centered over the region of campaign observation. The impact of SE data assimilation on model system forecasts was quantified through statistical assessment of the experiments (e.g., bias, root-mean-squared-error [RMSE], variable correlation) and direct comparison of model forecasts to TW13 measurements. These investigations focused on atmospheric quantities of direct relevance to EM refraction: temperature, moisture content and modified refractivity, as well as EM duct height and strength. New software codes were developed to illustrate the statistical results and model-measurement comparisons.

iii) *Adjoint-based observation impact on COAMPS error reduction*:
The COAMPS adjoint and tangent linear models predicted regions of optimal perturbation where the sensitivity to initial conditions of the modified refractivity vertical gradient in a pre-defined space was greatest. The COAMPS adjoint model was also used to investigate the relative impact of SE data assimilation on modified refractivity profile forecasts versus other assimilated observation datasets. Tests included assessment of the relative contribution to model forecast error reduction by UAS data assimilation at forecast lead times of 12 and 24 hours.

RESULTS

a. Scan Eagle data processing software development

The SE data processing software package was constructed to permit assimilation of SE data from the TW13 observation campaign into NAVDAS for use in generating COAMPS analyses. The package uses the First Guess at Appropriate Time (FGAT) assimilation technique to apply UAS observations at the most appropriate time within the NAVDAS 3D-Var data assimilation window. Further details on the development of this package can be found in the RTP UAS 2013 Report. Following its first operational use during the TW13 field campaign in July 2013, analysis of NAVDAS fields revealed several areas with potential for improvement. Corrections were made to the assimilation of UAS wind observations. The UAS time averaging routines were adjusted to average 1 Hz data over a 60 s window during level-flying and over a 10 s window during ascending and descending flight paths. The software was also modified to prevent automatic thinning of SE observations. Following the distribution of a quality-controlled version of the TW13 SE dataset to investigators in early 2014, the SE data processing software was updated to make use of new quality control flags for proper handling of the dataset. The updated SE data processing software package was used in conjunction with the quality controlled SE dataset during the re-runs of the COAMPS-NCOM model system TW13 experiments. Model fields at analysis time show examples of noticeable correction of temperature, moisture and

wind speed due to SE assimilation. Figure 2 illustrates impact of assimilation of SE wind speed measurements on the COAMPS-NCOM model analysis during TW13 experiments, comparing the background (first-guess) field to the observed values and the COAMPS analysis. The software package has since been applied to other projects as a foundation for UAS data assimilation algorithms.

b. Evaluation of COAMPS model performance during TW13

Verification of COAMPS model forecasts was computed using quality controlled observations taken during the TW13 campaign and from an adjacent WMO climate station. Verification of model vertical profiles used radiosonde measurements (50 during TW13 plus one climate station: WMO ID 72402). Verification at individual points in model space used SE flight observations (Case *noUAS* only). An assessment of the observed synoptic and mesoscale meteorology, using TW13 campaign measurements, local radiosonde measurements and remote sensing imagery, assisted in the interpretation and verification of model forecasts. Modified refractivity derived from observations provided useful information on the evolution of ducts and duct types.

Meteorological evaluation focused on temperature and dew point temperature. For profile comparisons, COAMPS forecasts with a six-hour cycle and lead times in hourly increments from zero to 24 hours were bi-linearly interpolated in the horizontal to each radiosonde launch location. Radiosondes were compared against all available model forecasts valid within 30 minutes of the launch. For point comparisons, these same COAMPS forecasts were interpolated horizontally and vertically to the location of one-minute averaged SE data from the seven flights extending up to 1500 m ASL. Case *noUAS* results suggested a broad net cold bias (~ -0.5°C) across most all vertical levels (Figure 3) with a temperature RMSE around 1°C. A net dry bias just above the model estimated ABL depth (~ -0.8°C bias in dew point temperature) is also found (Figure 3) and may be associated with missing cloud cover in the model forecasts. No clear moisture bias was identified within the ABL. Well above the ABL, verification from radiosondes supports a broad net moist bias (> 2°C) (Figure 3). Dew point temperature RMSE varied from around 1-2°C within the ABL to 4°C in the upper regions of SE measurement. In case *UAS* a broad reduction in RMSE in the vertical vicinity of SE measurements was found for both temperature and dew point temperature at forecast lead times as long as 12 hours. The RMSE reduction in these regions is found to be approximately 1°C and 1-3°C, respectively, with respect to case *noUAS* (Figure 4). Investigation into model performance during individual SE flights reveals local changes of up to 3 (8) °C in temperature (dew point temperature) versus the case *noUAS* forecasts, in most cases serving to mitigate bias from case *noUAS*. The improvements demonstrated across different flights also infer versatility in the SE assimilation technique (Figures 5, 6); which reduces biases resulting from varied sources of model error (e.g., cloud presence/absence, timing of front/trough passage).

Evaluation of COAMPS model performance with respect to EM propagation prediction concentrated on verification of modified refractivity profiles and ducting events, comparing cases *UAS* and *noUAS*. Mean profiles of modified refractivity derived from COAMPS forecasts at model grid points nearest to the location of the TW13 radiosonde launches were compared for cases *UAS* and *noUAS* using grids 3 and 4. Similarly the meteorological results, scores of modified refractivity RMSE reflect improvement in grid 4 in the lowest kilometer for short term forecasts (lead times from zero to six hours). Improvement in grid 3 and at longer lead times in grid 4 was found above 500 m ASL (Figure 7). Ducting event statistics were diagnosed using a contingency table to quantify the rate of false alarm,

correct null, hits and misses. Predicted propagation loss for an X-band radar, derived from COAMPS forecasts in case *noUAS*, matched well the loss derived from radiosonde measurements and captured the change in ducting behavior from weak, thin, elevated ducts to thicker, surface based ducts around 16 July 2013 (Figure 8). Ducts diagnosed from case *UAS* model results yielded duct top heights and thicknesses closer to the observed duct characteristics (based on radiosonde measurements) than those from case *noUAS* (Figure 9). This improvement in case *UAS* was found to be consistent over the duration of the TW13 observation campaign.

c. Adjoint-based observation impact on COAMPS error reduction

Testing of the COAMPS adjoint model in the TW13 observing region revealed the importance of accurately observing the low-level water vapor and temperature (see the RTP UAS 2013 Report for further details). Building on these results, additional experiments were conducted with the COAMPS observation impact system in order to further quantify forecast improvement associated with UAS observation assimilation. The observation impact system maps COAMPS adjoint sensitivity fields into observation space using the adjoint of NAVDAS and is used to determine an observation's influence in reducing forecast error. For these experiments both 12 hr and 24 hr forecast error in modified refractivity space was calculated over the area indicated by the box in Figure 10a in the lowest 1 km of the model's domain. The forecast error was used to force the COAMPS adjoint integrations. The resulting sensitivity fields were passed to the NAVDAS adjoint model to produce observation impacts. Also shown in Figure 10 are the cumulative impacts for the main observation types assimilated by NAVDAS. For the 12 hr experiment, the UAS observations had an overwhelming influence in reducing short term low level modified refractivity forecast errors (Figure 10b). Almost 60% of the error reduction is due to the UAS observations. Furthermore, dividing the cumulative impacts by the total number of each observation type further underscores the influence of the limited number of UAS observations in this area (Figure 10c). Evaluation of the impact of individual assimilated SE observations on forecast error reduction revealed that approximately 65 percent of the SE observations yielded error reduction in the 12 hr experiment. This exceeds the typical rate of 50 – 55 percent for other observation types The UAS observations remain beneficial in the 24 hr experiment (Figure 10d), especially on a per observation basis (Figure 10e), but not to the same extent they were for the 12 hr case. This result is consistent with the findings in the COAMPS model verification work.

RELATED PROJECTS

COAMPS will be used in related 6.1 projects within PE 0601153N that include studies of air-ocean coupling and boundary layer studies, and in related 6.2 projects within PE 0602435N that focus on the development of the atmospheric components (QC, analysis, initialization, and forecast model) of COAMPS. Developments in model post-processing software concerning the diagnosis and analysis of fields relevant to EM propagation prediction generated for this work are also currently in use by the SPAWAR-funded "Validation of tactical-scale EM propagation: COAMPS:EM" project and will likely also extend to the NRL-BASE funded "Boundary Layer Characterization for EM Propagation Predictions" project. This synergy of tool development among projects involving EM propagation serves to harmonize and expedite products for research and operational use.

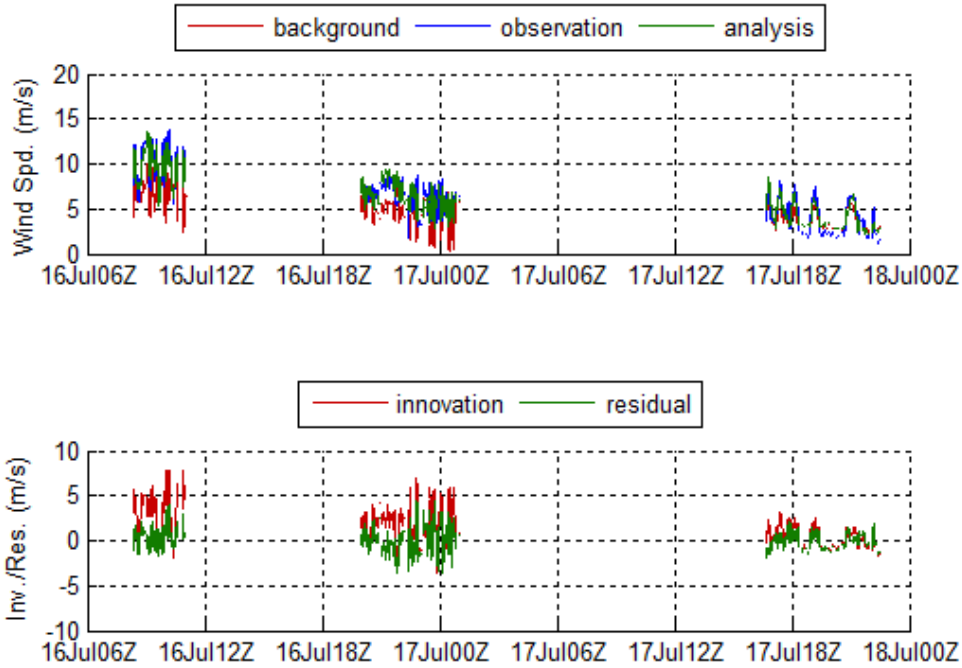

Figure 1. COAMPS model domains and horizontal grid sizes in Trident Warrior 2013 simulations.

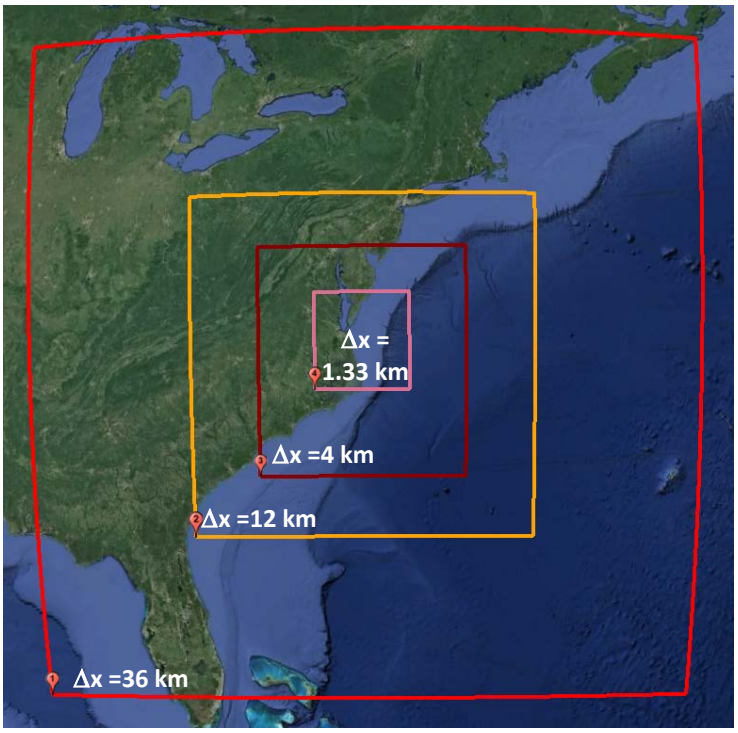

Figure 2. NAVDAS 3D-Var vectors for background (red), observed (blue) and analysis (green) wind speed assimilating observations from the ScanEagle UAS flights during the Trident Warrior 2013 campaign (top). The wind speed innovation vector (observation minus background) and residual vector (observation minus analysis) for the assimilated UAS observations (bottom).

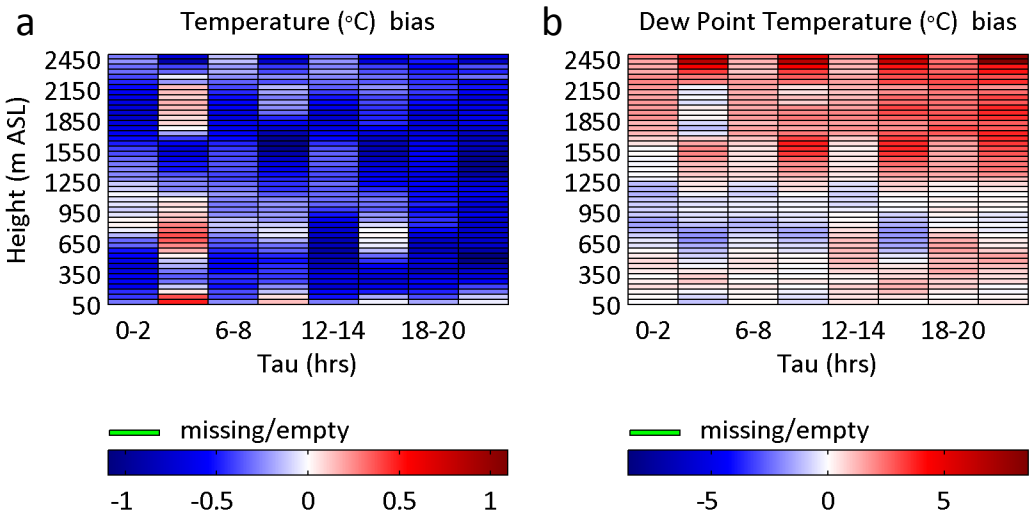

Figure 3. Bias of temperature (a) and dew point temperature (b) in case noUAS. Bias is calculated from all available model-measurement comparisons using Trident Warrior 2013 radiosonde measurements, organized into vertical bins representing geometric height above sea level. The forecast lead times (Tau) are merged together into bins of three-hours, labelled along the abscissa.

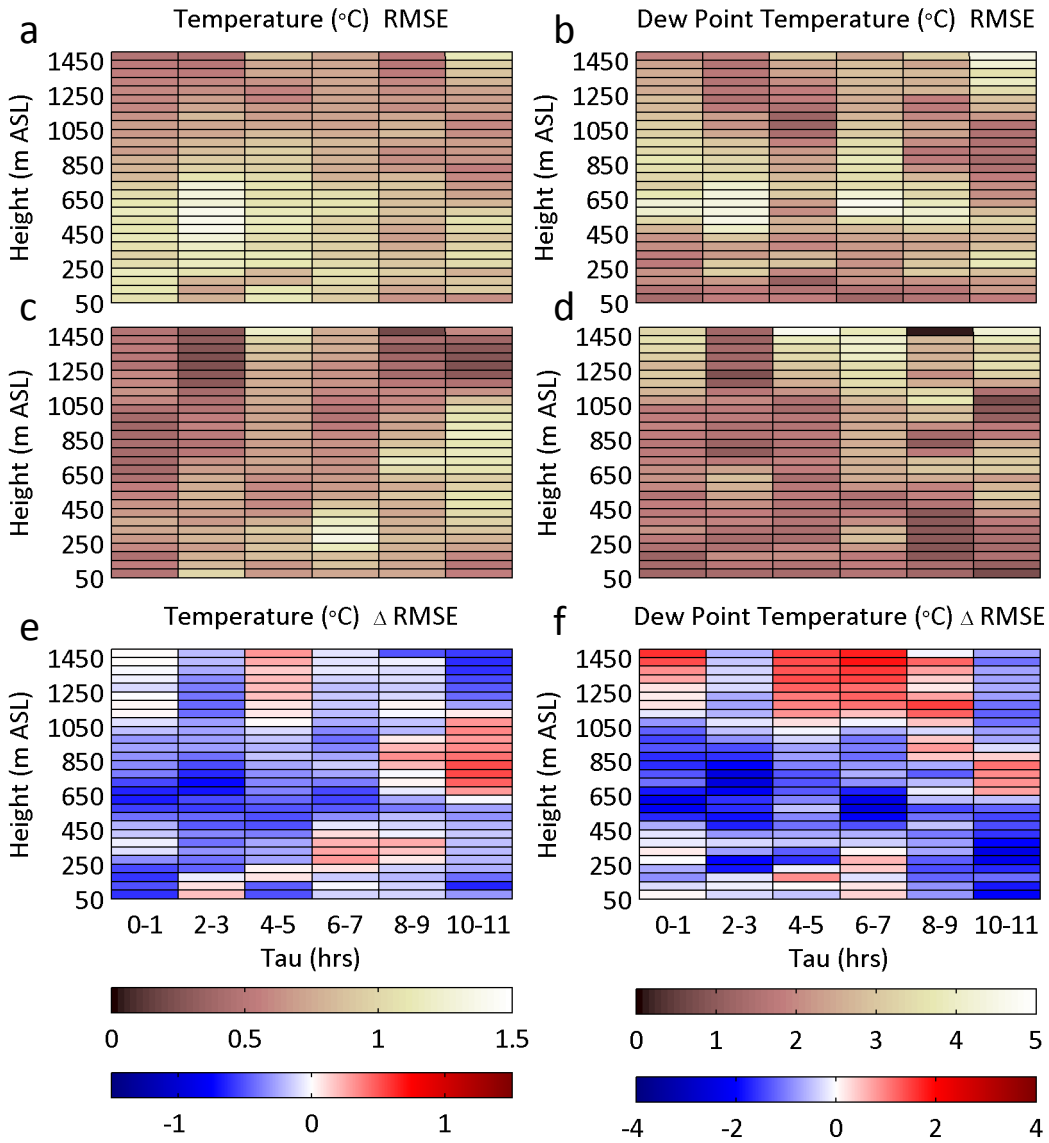

Figure 4. Root-mean-squared-error (RMSE) of temperature (a, c) and dew point temperature (b, d) in case noUAS (a, b) and case UAS (c, d). RMSE is calculated from all available model-measurement comparisons within vertical bins representing geometric height above sea level. The forecast lead times (Tau) are merged together into bins of two-hours, labelled along the abscissa of each subplot. The difference in RMSE between case UAS and case noUAS is shown for temperature (e) and dew point temperature (f).

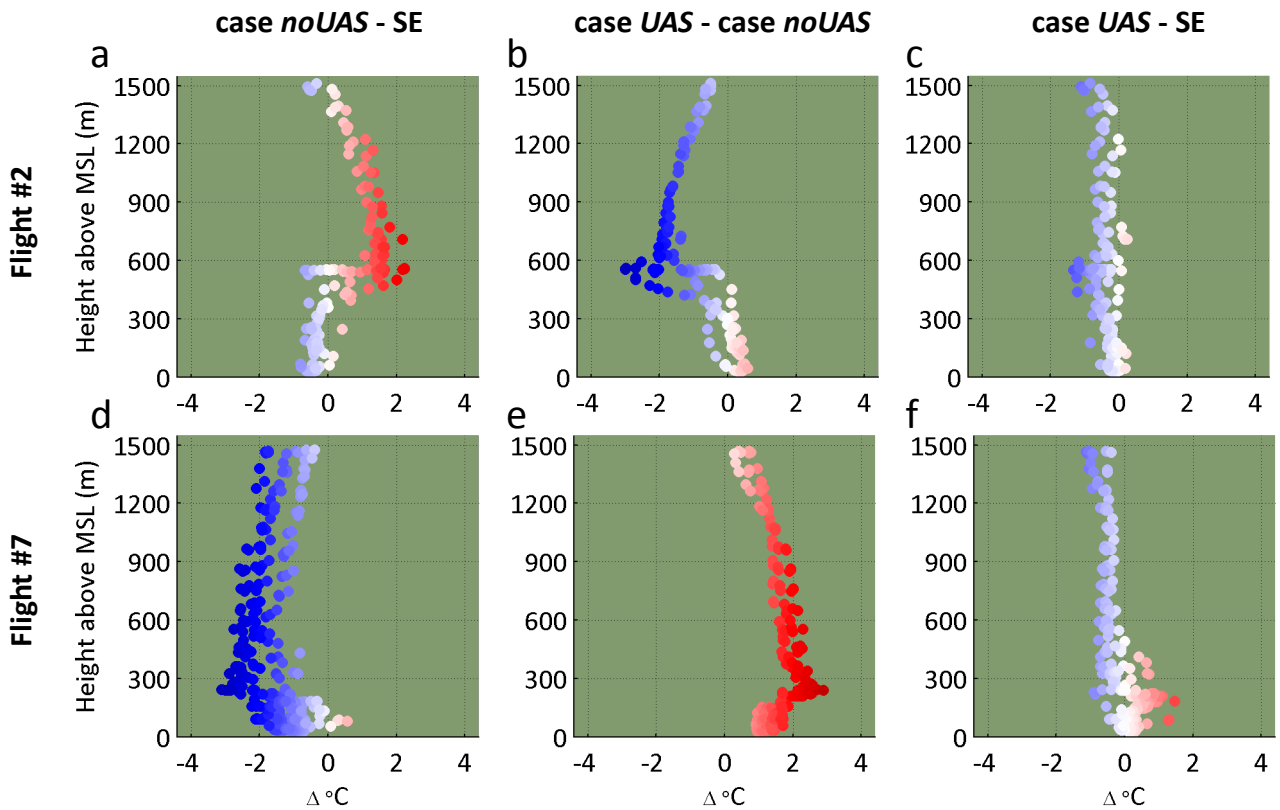

Figure 5. Difference of temperature computed along the flight paths of ScanEagle UAS Flight #2 (a)-(c) and #7 (d)-(f). Differences correspond to model-measurement using COAMPS case noUAS and SE measurements (a,d) [i.e. verification of case noUAS], COAMPS case UAS minus COAMPS case noUAS (b, e) and the sum of left two columns (c, f) [i.e., verification of case UAS]. COAMPS fields are taken from the nearest available forecast time ($0 \leq \tau \leq 5$ h).

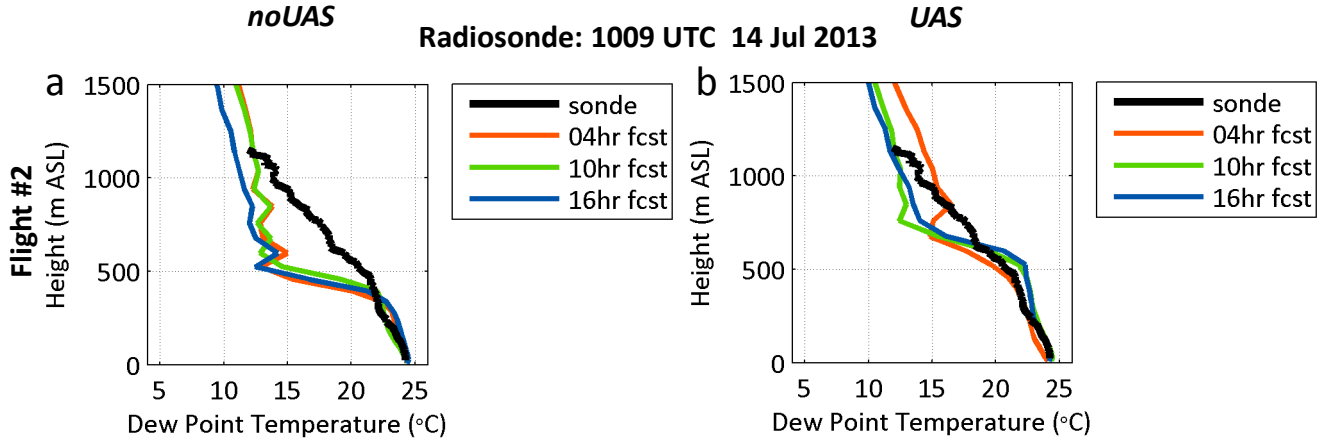

Figure 6. Comparison of a radiosonde measurement (black) versus COAMPS forecasts (colors) of dew point temperature during ScanEagle flight #2 for the noUAS (a) and UAS (b) cases. Forecast data are taken from the nearest hour, allowing for up to a 30 minute difference between the time of measurement and forecast.

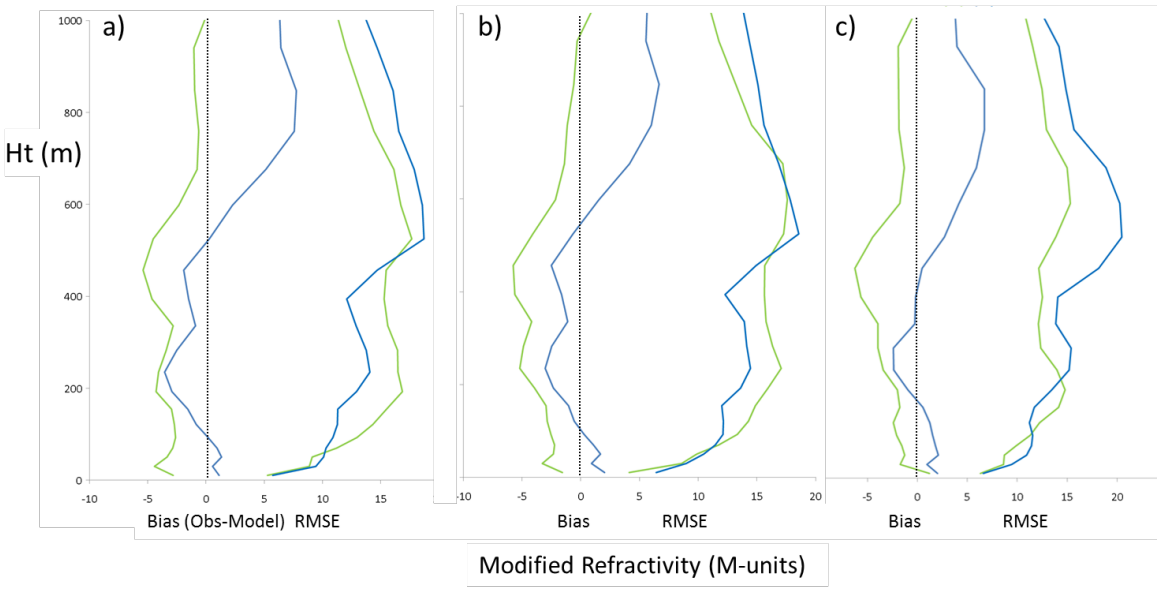

Figure 7. Comparison of modified refractivity bias (observation minus model) and RMSE for case noUAS (blue) and case UAS (green) simulations using grids 3 (a) and 4 (b, c),for forecast lead times 1-12 hrs, (a, b) and 1-6 hrs (c).

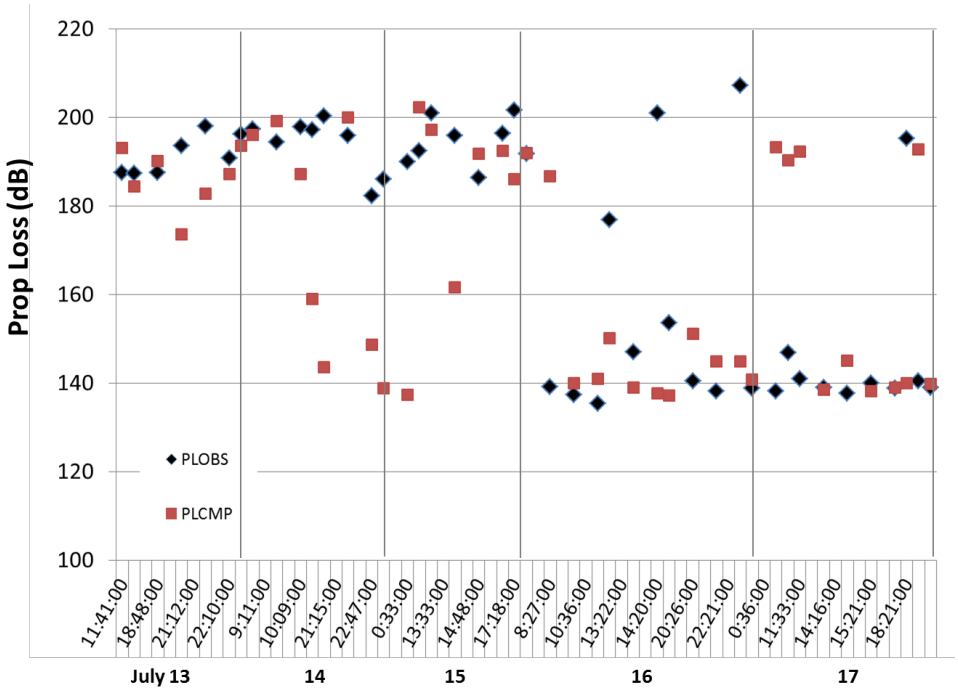

Figure 8. Comparison of the propagation path loss (dB; at height of 5 m, 27.5 km down range of VACAPES (east)) over the five day TW 13 observing campaign for an X-band radar at a height of 15 m using the modified refractivity profile computed from radiosonde measurements (black symbols), from the nearest COAMPS grid point forecast from case noUAS (red symbols).

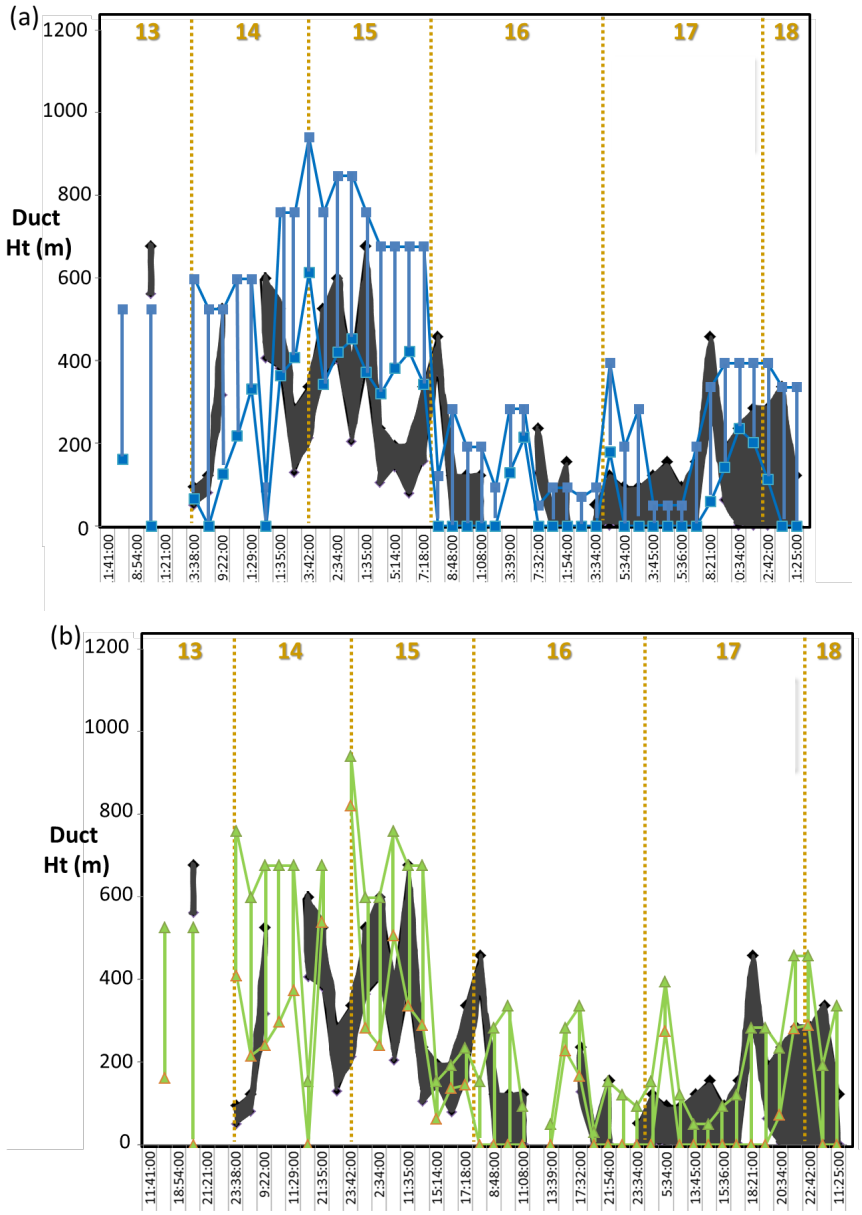

Figure 9. Concatenated time-series of the duct layer computed from radiosonde measurements (grey symbols) compared to case noUAS (a) and case UAS (b). The grey shaded region represents the observed duct layer thickness and depth. The blue and green lines show the trend in the simulated duct layer over the five day period with dates shown in yellow along the top and times (UTC) along the abscissa.

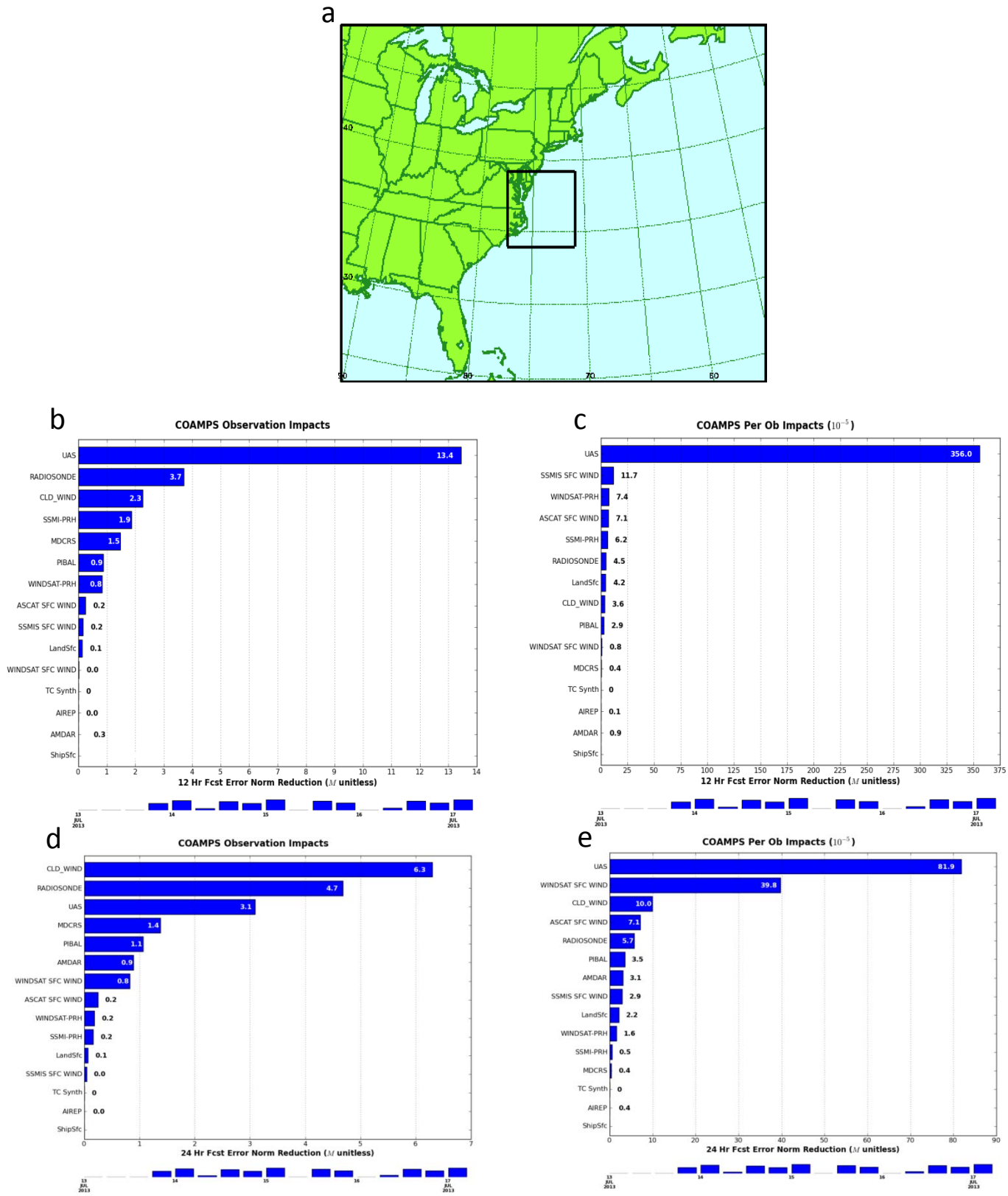

Figure 10. COAMPS observation impacts in modified refractivity space for each observation type assimilated by NAVDAS for the 12 hr forecast (b) and 24 hr forecast (d) experiments. The forecast error was calculated in the area indicated by the box in (a) in the lowest 1 km. Impacts were divided by the number of observations per type in (c) [12 hr] and (e) [24 hr].